Estimates for the single-spin asymmetries in the $p^{\uparrow}p \to J/\psi X$ process at PHENIX RHIC and SPD NICA

A. V. Karpishkov[*] and V. A. Saleev[†]

Samara National Research University, Moskovskoe Shosse, 34, 443086 Samara, Russia and Joint Institute for Nuclear Research, Dubna 141980, Russia

M. A. Nefedov[‡]

Samara National Research University, Moskovskoe Shosse, 34, 443086 Samara, Russia

(Received 18 August 2020; accepted 18 June 2021; published 7 July 2021)

We study the transverse single-spin asymmetry (TSSA) in $p^{\uparrow}p \to J/\psi X$ reaction, incorporating both transverse momentum and spin effects. To predict production cross section of prompt J/ψ, we use two different approaches, the color-singlet model and the improved color evaporation model, and show how the predicted results for TSSAs depend on the choice of hadronization model. For initial-state factorization, we also consider two options: the standard generalized parton model and the color gauge-invariant version of it. Estimates for the TSSAs in $p^{\uparrow}p \to J/\psi X$ process for the conditions of the future Spin Physics Detector Nuclotron-based Ion Collider fAcility (NICA) experiment are presented for the first time.

DOI: 10.1103/PhysRevD.104.016008

I. INTRODUCTION

The transverse momentum dependent (TMD) parton distribution functions (PDFs) incorporate information about the three-dimensional structure of a proton and its spin properties [1,2]. Among the leading-twist TMD PDFs, the Sivers function [3,4] is one of the most interesting functions and it is widely investigated in $p^{\uparrow}p \to hX$ inclusive processes [5,6]. The Sivers function describes the number density of unpolarized gluons g (or quarks q) with the intrinsic transverse momentum $\mathbf{q}_T$ inside a transversely polarized proton $p^{\uparrow}$, with the three-momentum $\mathbf{P}$ and the spin polarization vector $\mathbf{S}$,

$$F_g^{\uparrow}(x, \mathbf{q}_T) = F_g(x, q_T) + \frac{1}{2}\Delta^N F_g^{\uparrow}(x, q_T)\mathbf{S} \cdot (\hat{\mathbf{P}} \times \hat{\mathbf{q}}_T), \quad (1)$$

where x is the proton light-cone momentum fraction carried by the gluon, $F_g(x, q_T)$ is the unpolarized TMD parton density, $\Delta^N F_g^{\uparrow}(x, q_T)$ is the Sivers function, $q_T = |\mathbf{q}_T|$, and the symbol $\hat{(\ )}$ denotes a unit vector, $\hat{\mathbf{a}} = \mathbf{a}/|\mathbf{a}|$.

In the present paper, we are interested in accessing the gluon Sivers function (GSF) using the TSSA of inclusive J/ψ production. However, the task of studying gluon distributions using charmonia is rather challenging theoretically. The production of charmonia proceeds in two stages: first, a $c\bar{c}$ pair is produced at short distances, predominantly via gluon-gluon fusion but with a non-negligible contribution of $q\bar{q}$- and qg-initiated subprocesses. The second stage is hadronization of the $c\bar{c}$ pair into a physical charmonium state, which proceeds essentially nonperturbatively, at large distances (low scales) and is accompanied by a complicated rearrangement of color via exchanges of soft gluons between the $c\bar{c}$ pair and other colored partons produced in the collision. At present, two approaches to describe $c\bar{c}$ hadronization are most popular: the nonrelativistic QCD (NRQCD) factorization [7] and (improved) color evaporation model (CEM) [8–10].

In the context of TMD factorization, rigorous results for heavy-quarkonium physics were obtained only very recently [11,12], showing that the TMD-factorization formula for quarkonium production will differ from the case of Drell-Yan pair or Higgs-boson production processes. For quarkonia, the TMD-factorization formula has to include additional shape functions with the corresponding evolution. However, in the present paper, we adopt a simpler phenomenological approach of generalized parton model (GPM) which is described in more detail in Sec. II A. In the standard GPM approach, the Sivers function is assumed to be process dependent, because the effects of initial-state interaction (ISI) and final-state interaction (FSI) are factorized into this function. An alternative approach is the

[*]karpishkoff@gmail.com
[†]saleev@samsu.ru
[‡]nefedovma@gmail.com

color-gauge-invariant (CGI) GPM formalism of Refs. [13–18], which we summarize in Secs. II B and II C. In this framework, the process-dependent ISIs and FSIs are lifted from Sivers-like TMD PDF to the coefficient function, using the one-gluon exchange approximation. Thus, in CGI-GPM, the results for the Sivers function extracted from different processes can be directly compared.

The behavior of TSSA in the process $p^\uparrow p \to J/\psi X$ has been studied recently in Refs. [16,17,19]. In Refs. [16,17], J/ψ production was treated in a color-singlet approximation [16] and full NRQCD approach [17], including the color-octet states, respectively. In case of the color-singlet mechanism, the CGI-GPM corrections to GPM cross sections have been included. In Ref. [19], the improved color evaporation model (ICEM) was used and the authors investigated the effect of the evolution of TMD PDFs involved on the asymmetry A_N.

The aim of the present study is to provide reasonable estimates for TSSA effects which can be observed in the kinematic conditions of the planned Spin Physics Detector (SPD) experiment at NICA collider [20,21]. We will compare the estimates for TSSA obtained in GPM and CGI-GPM frameworks and also explore both the theoretical approaches for charmonium hadronization—NRQCD and ICEM. In case of NRQCD, we will show that at small transverse momenta of the produced charmonium $k_{T\mathcal{C}} < m_{\mathcal{C}}$, the color-singlet mechanism describes data for prompt J/ψ production and the inclusion of color-octet terms is not needed at leading order (LO) in α_s. Therefore, for our NRQCD predictions for TSSA within GPM and CGI-GPM, we include only the color-singlet states of the final $c\bar{c}$ pair.

The present paper is organized as follows. In Sec. II, we present basic cross section formulas of GPM and CGI-GPM for $2 \to 1$ and $2 \to 2$ partonic subprocesses, as well as the details specific to our NRQCD/color-singlet model (CSM) and ICEM treatments of charmonium hadronization. In Sec. III, we present and discuss numerical results for the transverse momentum spectra of prompt J/ψ and TSSA A_N in $p^\uparrow p \to J/\psi X$ reactions at PHENIX RHIC and Spin Physics Detector (SPD) Nuclotron-based Ion Collider fAcility (NICA). In this section, we also compare our results with the similar results obtained earlier for PHENIX RHIC at $\sqrt{s} = 200$ GeV in both NRQCD approach [16,17] and ICEM [19].

II. THEORETICAL FORMALISM

A. GPM and CGI-GPM

The factorization scheme, which is suitable to describe inclusive observables in hadronic collisions, depends on hierarchy between the typical hard scale of the process and the involved transverse momenta. Collinear parton model (CPM) is used for studies of high-p_T production, when hard scale ($\mu \sim p_T \gg \Lambda_{\rm QCD}$). In such a way, in CPM, we neglect the transverse momenta of partons initiating the hard process and the hadronic cross section can be factorized as convolution of hard coefficients and collinear PDFs $f_a(x,\mu_F)$ at the factorization scale μ_F with $\mu_F \simeq \mu \sim p_T$ and $a = q, \bar{q}, g$. In the kinematical domain of CPM, the transverse momenta of final-state particles ($\mathbf{k}_T$) are generated in the hard scattering of partons and influence small intrinsic transverse momenta of partons in hadrons ($\mathbf{q}_T$), which originate from nonperturbative effects, which can be neglected. The typical estimate for average squared intrinsic transverse momentum of a parton is $\langle \mathbf{q}_T^2 \rangle \simeq 1$ GeV^2 or even smaller.

If one is interested in the particle production with small transverse momenta $|\mathbf{k}_T| \simeq \sqrt{\langle \mathbf{q}_T^2 \rangle} \ll \mu$ in a hard process with the scale μ, the effects of the intrinsic parton motion in hadrons have to be taken into account. In TMD factorization, the hadronic cross section is expressed as a convolution of TMD PDFs $F_a(x, q_T, \mu, \zeta)$ and hard partonic cross section. TMD PDFs evolve with respect to two scales: μ and ζ, where the latter one is the so-called rapidity scale related with rapidity divergences [22]. The typical value of the hard scale μ in charmonium ($\mathcal{C}$) production is given by the charmonium mass, $m_{\mathcal{C}} = 3.1$–3.7 GeV, so TMD factorization should be used in the region $k_T \ll m_{\mathcal{C}}$. The region $k_T \simeq m_{\mathcal{C}}$ requires matching with finite-order perturbative corrections and possible nonperturbative power-suppressed corrections to the TMD term.

The GPM is a simplified version of TMD factorization, which is generally applied for phenomenological estimates of various observables in processes for which TMD factorization has not been rigorously proven yet. Typically, TMD PDFs in GPM are parametrized by a simple factorized prescription which is as follows:

$$F_a(x, q_T, \mu_F) = f_a(x, \mu_F) G_a(q_T), \tag{2}$$

where $f_a(x,\mu_F)$ is the corresponding collinear PDF. The dependence on the transverse momentum of a parton is described by Gaussian distribution $G_a(q_T) = \exp[-q_T^2/\langle q_T^2 \rangle_a]/(\pi \langle q_T^2 \rangle_a)$, with the normalization condition $\int d^2 q_T G_a(q_T) = 1$. The effects of TMD evolution with respect to the rapidity scale [22,23] ζ are neglected, which means that GPM estimates are applicable only in a narrow range of hard and rapidity scales $\zeta \sim \mu$. The latter condition is however always fulfilled in our case, since the scale of the process of charmonium production at low $k_{T\mathcal{C}}$ is given by $m_{\mathcal{C}}$.

Within the GPM, the differential cross section for the charmonium production in proton-proton collisions can be written as follows:

$$d\sigma(pp \to \mathcal{C}X) = \int dx_1 \int d^2\mathbf{q}_{1T} \int dx_2 \times \int d^2\mathbf{q}_{2T} F_g(x_1, \mathbf{q}_{1T}, \mu_F) F_g(x_2, \mathbf{q}_{2T}, \mu_F) d\hat{\sigma}, \tag{3}$$

where $d\hat{\sigma}$ is the partonic cross section for $gg \to \mathcal{C}$ or $gg \to \mathcal{C} + g$ partonic subprocesses. For the $2 \to 1$-type hard subprocess $g(q_1) + g(q_2) \to \mathcal{C}(k)$, one has

$$d\hat{\sigma}(gg \to \mathcal{C}) = (2\pi)^4 \delta^{(4)}(q_1 + q_2 - k) \frac{\overline{|M(gg \to \mathcal{C})|^2}}{2x_1 x_2 s} \frac{d^4k}{(2\pi)^3} \delta_+(k^2 - m_{\mathcal{C}}^2), \tag{4}$$

with $s = 2P_1P_2$—the squared center-of-mass energy of the pp collision. Integrating out delta functions, one obtains

$$\frac{d\sigma(pp \to \mathcal{C}X)}{d^2k_T} = \frac{\pi}{s} \int \frac{dx_1}{x_1} \int d^2q_{1T} \int \frac{dx_2}{x_2} F_g(x_1, \mathbf{q}_{1T}, \mu_F) F_g(x_2, \mathbf{q}_{2T}, \mu_F) \overline{|M(gg \to \mathcal{C})|^2} \delta(\hat{s} - m_{\mathcal{C}}^2), \tag{5}$$

where $\hat{s} = k^2 = (q_1 + q_2)^2$, $\mathbf{q}_{2T} = \mathbf{k}_T - \mathbf{q}_{1T}$, $k^\mu = (k_0, \mathbf{k}_T, k_z)^\mu$. For the consistency of GPM and to avoid problems with the gauge invariance of the hard-scattering amplitudes, the four-momenta of the initial-state partons have to be put on mass shell ($q_1^2 = q_2^2 = 0$). Hence, $q_{1,2}$ read

$$q_1^\mu = \left(x_1 \frac{\sqrt{s}}{2} + \frac{\mathbf{q}_{1T}^2}{2\sqrt{s}x_1}, \mathbf{q}_{1T}, x_1 \frac{\sqrt{s}}{2} - \frac{\mathbf{q}_{1T}^2}{2\sqrt{s}x_1} \right)^\mu, \tag{6}$$

$$q_2^\mu = \left(x_2 \frac{\sqrt{s}}{2} + \frac{\mathbf{q}_{2T}^2}{2\sqrt{s}x_2}, \mathbf{q}_{2T}, -x_2 \frac{\sqrt{s}}{2} + \frac{\mathbf{q}_{2T}^2}{2\sqrt{s}x_2} \right)^\mu, \tag{7}$$

where $x_{1,2}$ are the proton light-cone momentum fractions carried by the partons

$$x_1 = \frac{q_1^0 + q_1^3}{\sqrt{s}}, \qquad x_2 = \frac{q_2^0 - q_2^3}{\sqrt{s}}.$$

As follows from Eqs. (6) and (7),

$$\hat{s} = x_1 x_2 s + 2\mathbf{q}_{1T}^2 - 2|\mathbf{q}_{1T}||\mathbf{k}_T| \cos(\phi_1) + \frac{\mathbf{q}_{1T}^2 \mathbf{q}_{2T}^2}{x_1 x_2 s}. \tag{8}$$

The latter result allows one to integrate out delta function $\delta(\hat{s} - m_{\mathcal{C}}^2)$ taking the integral over dx_2 in Eq. (5). To perform the calculation of the transverse momentum spectrum in a fixed rapidity interval, one inserts a Heaviside theta function implementing the rapidity cut under the sign of the integral (5), while the rapidity of $\mathcal{C}$ can be calculated as

$$y = \ln\left(\frac{k^0 + k^3}{m_{\mathcal{C}T}} \right), \qquad m_{\mathcal{C}T} = \sqrt{m_{\mathcal{C}}^2 + k_T^2}, \qquad k^0 + k^3 = x_1\sqrt{s} + \frac{q_{2T}^2}{x_2\sqrt{s}}.$$

The cross section for the $2 \to 2$ subprocess $g(q_1) + g(q_2) \to \mathcal{C}(k) + g(q_3)$ is given by the formula (3) with

$$d\hat{\sigma}(gg \to \mathcal{C}g) = (2\pi)^4 \delta^{(4)}(q_1 + q_2 - k - q_3) \frac{\overline{|M(gg \to \mathcal{C}g)|^2}}{2x_1 x_2 s} \frac{d^3k}{(2\pi)^3 2k_0} \frac{d^4q_3}{(2\pi)^3} \delta_+(q_3^2). \tag{9}$$

Replacing $q_3^2 \to \hat{s} + \hat{t} + \hat{u} - m_{\mathcal{C}}^2$ with $\hat{t} = (q_1 - k)^2$, $\hat{u} = (q_2 - k)^2$, one can remove the integral over d^4q_3 by the delta function and obtain

$$k_0 \frac{d\sigma}{d^3k} = \frac{d\sigma}{dy d^2k_T} = \frac{1}{16\pi^2} \int dx_1 \int d^2q_{1T} \int dx_2 \int d^2q_{2T} F_g(x_1, \mathbf{q}_{1T}, \mu_F) F_g(x_2, \mathbf{q}_{2T}, \mu_F) \times \frac{\overline{|M(gg \to \mathcal{C}g)|^2}}{x_1 x_2 s} \delta(\hat{s} + \hat{t} + \hat{u} - m_{\mathcal{C}}^2), \tag{10}$$

where

$$\hat{t} = m_{\mathcal{C}}^2 - \sqrt{s} m_{\mathcal{C}T} x_1 e^{-y} - \frac{\mathbf{q}_{T1}^2 m_{\mathcal{C}T} e^{y}}{\sqrt{s} x_1} + 2|\mathbf{q}_{T1}||\mathbf{k}_T|\cos(\phi_1),$$

$$\hat{u} = m_{\mathcal{C}}^2 - \sqrt{s} m_{\mathcal{C}T} x_2 e^{y} - \frac{\mathbf{q}_{T2}^2 m_{\mathcal{C}T} e^{-y}}{\sqrt{s} x_2} + 2|\mathbf{q}_{T2}||\mathbf{k}_T|\cos(\phi_2).$$

Then one can take the integral over dx_2 analytically using the delta function $\delta(\hat{s} + \hat{t} + \hat{u} - m_C^2)$. In such a way, no kinematic approximations are made and the exact $2 \to 1$ and $2 \to 2$ kinematics are implemented in the presence of the transverse momentum of initial-state partons.

Master formulas presented above have been used directly in calculations of prompt J/ψ production in the NRQCD approach; see Sec. II B for a description of the contributing $2 \to 1$ and $2 \to 2$ partonic subprocesses. In the case of ICEM hadronization model, the cross section is calculated in a slightly different way; see Sec. II C.

In this paper, we study TSSAs, usually denoted by A_N, measured in $p^\uparrow p \to \mathcal{C}X$ ($\mathcal{C} = J/\psi, \chi_c, \psi(2S)$) inclusive reactions and defined as

$$A_N = \frac{d\sigma^\uparrow - d\sigma^\downarrow}{d\sigma^\uparrow + d\sigma^\downarrow} = \frac{d\Delta\sigma}{2d\sigma}, \tag{11}$$

where $\uparrow, \downarrow$ are opposite proton spin orientations perpendicular to the scattering plane in pp center-of-mass frame. The numerator and denominator of A_N read

$$d\Delta\sigma \propto \int dx_1 \int d^2q_{1T} \int dx_2 \int d^2q_{2T} [\hat{F}_g^\uparrow(x_1, \mathbf{q}_{1T}, \mu_F) - \hat{F}_g^\downarrow(x_1, \mathbf{q}_{1T}, \mu_F)] F_g(x_2, \mathbf{q}_{2T}, \mu_F) d\hat{\sigma}(gg \to \mathcal{C}X), \tag{12}$$

$$d\sigma \propto \int dx_1 \int d^2q_{1T} \int dx_2 \int d^2q_{2T} F_g(x_1, \mathbf{q}_{1T}, \mu_F) F_g(x_2, \mathbf{q}_{2T}, \mu_F) d\hat{\sigma}(gg \to \mathcal{C}X), \tag{13}$$

where $\hat{F}_g^{\uparrow,\downarrow}(x, q_T, \mu_F)$ is the distribution of the unpolarized gluon (or quark) in a polarized proton. Following the Trento conventions [24], the GSF can be introduced as

$$\begin{aligned}\Delta\hat{F}_g^\uparrow(x_1, \mathbf{q}_{1T}, \mu_F) &\equiv \hat{F}_g^{(\uparrow)}(x_1, \mathbf{q}_{1T}, \mu_F) - \hat{F}_g^{(\downarrow)}(x_1, \mathbf{q}_{1T}, \mu_F) \\ &= \Delta^N F_g^\uparrow(x_1, \mathbf{q}_{1T}^2, \mu_F)\cos(\phi_1) = -2\frac{q_{1T}}{M_p} F_{1T}^g(x_1, q_{1T}, \mu_F)\cos(\phi_1),\end{aligned} \tag{14}$$

and GSF has to satisfy the positivity bound

$$\frac{q_{1T}}{M_p}|F_{1T}^g(x_1, q_{1T}, \mu_F)| \le F_g(x_1, q_{1T}, \mu_F), \tag{15}$$

where M_p is the mass of the proton.

We adopt factorized Gaussian parametrizations for both the unpolarized TMD distribution $F_g(x, q_T, \mu_F)$ and the Sivers function $\Delta^N F_g^\uparrow(x, q_T^2, \mu_F)$,

$$\Delta^N F_g^\uparrow(x, q_T^2, \mu_F) = 2N_g(x) F_g(x, q_T, \mu_F) h(q_T), \tag{16}$$

$$N_g(x) = N_g x^\alpha (1-x)^\beta \frac{(\alpha+\beta)^{\alpha+\beta}}{\alpha^\alpha \beta^\beta}, \tag{17}$$

$$h(q_T) = \sqrt{2e}\frac{q_T}{M'} e^{-q_T^2/M'^2}, \tag{18}$$

which satisfy the bound (15) for any values of α and β. After introducing the parameter

$$\rho_g = \frac{M'^2}{M'^2 + \langle q_T^2 \rangle_g}, \qquad 0 < \rho_g < 1, \tag{19}$$

TABLE I. Parameters of GSF.

GSF set	N_g	α_g	β_g	ρ_g	$\langle q_T^2\rangle_g$, GeV^2
SIDIS1	0.65	2.8	2.8	0.687	0.25
D'Alesio *et al.*	0.25	0.6	0.6	0.1	1.0

we write for GSF,

$$\Delta^N F_g^{\uparrow}(x,q_T^2,\mu_F) = 2\frac{\sqrt{2e}}{\pi}N_g(x)f_g(x,\mu_F)\sqrt{\frac{1-\rho_g}{\rho_g}}\frac{q_T}{\langle q_T^2\rangle_g^{3/2}}e^{-q_T^2/\rho_g\langle q_T^2\rangle_g}. \tag{20}$$

In our numerical calculations, we will use two different GSFs obtained earlier in Ref. [6], which we call semi-inclusive deep inelastic scattering (SIDIS1) for brevity, and in Ref. [25], which we refer to as GSF parametrization by D'Alesio *et al.* The corresponding values of the parameters are presented in Table I.

To introduce the CGI-GPM, let us first recall the explanation of the Sivers effect, which has been described for the first time in Ref. [26]. In this paper, it was shown that Sivers asymmetry in SIDIS process at a leading twist is a quantum effect generated by exchanges of soft gluons between ISI or FSI partons produced in a hard process and the spectator system originating as a remnant of an incoming hadron. In a standard TMD factorization, these soft gluons are taken into account within the gauge-invariant definition of Sivers-like TMD PDF, which contains Wilson lines. The sign of Sivers TMD PDF depends on the direction of Wilson lines, which can be past or future pointing, representing the "space-time trajectory" of an initial-state or struck quark produced, respectively, in Drell-Yan or SIDIS hard-scattering process. Thus, the Sivers function in a standard TMD and perhaps in GPM approaches is process dependent and it is not clear how to extend factorization for the Sivers effect to the processes with colored final states, like J/ψ production.

The aim of CGI-GPM [13–18] formalism is to extract the above-mentioned process dependence from the TMD PDF to the hard-scattering coefficient. The effects of ISI and FSI are included in CGI-GPM via one-gluon exchange approximation [13,16]. In the case of the gluon Sivers effect, this approximation leads to the appearance of independent GSFs of f type ($F_{1T}^{g(f)}$) and d type ($F_{1T}^{g(d)}$) corresponding to two independent ways of combining three gluons into a color singlet (Fig. 1). The coupling of additional "eikonal" gluon from the GSF to the hard process leads only to the modification of the color structure of the latter one. There is no four-momentum transfer from the additional gluon to the hard process, because the Sivers effect comes from the imaginary part of the loop integral over the momentum of the exchanged gluon [26], which is saturated by the contribution of the soft region. Moreover, only the coupling

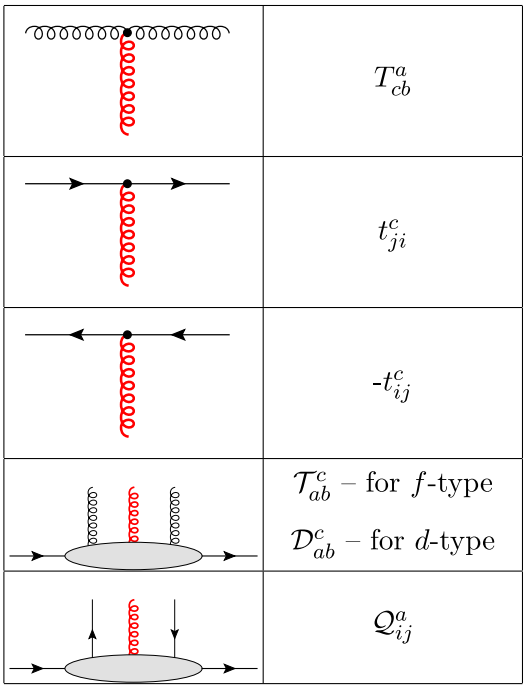

FIG. 1. Feynman rules for color factors within the CGI-GPM with the additional eikonal gluon.

of the eikonal gluon to the initial-state or *observed* colored final-state particles contributes to the spin asymmetry, while the effects of coupling to unobserved final-state partons cancel out between the amplitude and the complex-conjugate amplitude (see, e.g., discussion in Refs. [13,16]). While arguments above are specific for the one-gluon exchange approximation, an additional argument in favor of CGI-GPM is that its hard-scattering coefficients reproduce coefficients in the twist-3 collinear approach [13].

In Fig. 1, we collect the corresponding Feynman rules and prescriptions for calculation of the hard-scattering coefficient for the numerator (12) of the TSSA within CGI GPM. For a detailed derivation, see, e.g., Ref. [16]. The color projectors for f- and d-type GSFs are defined as follows:

$$\mathcal{T}^c_{ab} = \mathcal{N}_{\mathcal{T}}(-if_{abc}), \quad \mathcal{D}^c_{ab} = \mathcal{N}_{\mathcal{D}}d_{abc}, \quad \mathcal{Q}^a_{ij} = \mathcal{N}_{\mathcal{Q}}t^a_{ij}, \tag{21}$$

where $f_{abc}(d_{abc})$ is totally the antisymmetric (symmetric) structure constant of the $SU(N_c)$ color gauge group, t^a_{ij}—the generators of $SU(N_c)$ group in the fundamental representation, and

$$\mathcal{N}_{\mathcal{T}} = \frac{1}{N_c(N_c^2-1)}, \qquad \mathcal{N}_{\mathcal{D}} = \frac{N_c}{(N_c^2-4)(N_c^2-1)}, \qquad \mathcal{N}_{\mathcal{Q}} = \frac{2}{N_c(N_c^2-1)}, \tag{22}$$

with $N_c = 3$.

In the following sections, we mostly use the CGI-GPM hard-scattering coefficients, which already have been calculated by other authors, in which case we cite the corresponding reference. However, in Sec. II C, we will need new (to our knowledge) CGI-GPM hard-scattering coefficient for $gg \to c\bar{c}$ process with *both* final-state c quarks being observed.

B. NRQCD and color-singlet model

In the framework of the NRQCD-factorization approach, the cross section of charmonium production via a partonic subprocess $a + b \to \mathcal{C} + X$ is given by a double expansion in powers of α_s and squared relative velocity of heavy quarks in a bound state v^2 as

$$d\hat{\sigma}(a + b \to \mathcal{C} + X) = \sum_n d\hat{\sigma}(a + b \to c\bar{c}[n] + X)\langle \mathcal{O}^{\mathcal{C}}[n]\rangle, \tag{23}$$

where n denotes the set of color, spin, orbital, and total angular momentum quantum numbers of the $c\bar{c}$ pair and the four-momentum of the latter is assumed to be equal to the one of the physical quarkonium states $\mathcal{C}$. The cross section $d\hat{\sigma}(a + b \to c\bar{c}[n] + X)$ can be calculated in perturbative QCD as an expansion in α_s. The nonperturbative transition of the $c\bar{c}$ pair into $\mathcal{C}$ is described by the long-distance matrix elements (LDMEs) $\langle \mathcal{O}^{\mathcal{C}}[n]\rangle$. Color-singlet LDMEs can be determined from measured decay widths of charmonia using the known next-to-leading-order (NLO) QCD result or from calculations in potential models [27]. The color-octet LDMEs are considered as free parameters in charmonium production cross sections. Typically, LDMEs up to next-to-next-to-leading-order ($O(v^4)$) in v^2 scaling are included in NRQCD-factorization calculations: $n = {}^3S_1^{(1)}$, ${}^3S_1^{(8)}$, ${}^1S_0^{(8)}$, ${}^3P_J^{(8)}$ if $\mathcal{C} = J/\psi, \psi'$ and $n = {}^3P_J^{(1)}$, ${}^3S_1^{(8)}$ if $\mathcal{C} = \chi_{cJ}$, where $J = 0, 1, 2$.

From a general point of view, LDMEs should be universal and process-independent parameters. However, in practice, their numerical values strongly depend on the approach which is used to describe the $c\bar{c}$-pair production and data included into the fit. For example, one can compare the color-octet LDMEs obtained in LO CPM [28,29], NLO CPM [30], and k_T-factorization approach [31,32]. Nevertheless, the hierarchy expected from velocity-scaling rules $\langle \mathcal{O}^{\mathcal{C}}[{}^3P_0^{(1)}]\rangle \gg \langle \mathcal{O}^{\mathcal{C}}[{}^3P_0^{(8)}]\rangle$, $\langle \mathcal{O}^{\mathcal{C}}[{}^3S_1^{(1)}]\rangle \gg \langle \mathcal{O}^{\mathcal{C}}[{}^3P_J^{(8)}]\rangle \gg (\langle \mathcal{O}^{\mathcal{C}}[{}^3S_1^{(8)}]\rangle, \langle \mathcal{O}^{\mathcal{C}}[{}^1S_0^{(8)}]\rangle)$ is respected by all the fits.

We adopt the following values of color-singlet LDMEs [33]: $\langle \mathcal{O}^{J/\psi}[{}^3S_1^{(1)}]\rangle = 1.3\ \mathrm{GeV}^3$, $\langle \mathcal{O}^{\psi'}[{}^3S_1^{(1)}]\rangle = 6.5 \times 10^{-1}\ \mathrm{GeV}^3$, and $\langle \mathcal{O}^{\chi_{cJ}}[{}^3P_0^{(1)}]\rangle = 8.9 \times 10^{-2}\ \mathrm{GeV}^5$ and LDMEs for other P-wave color-singlet states are obtained via the heavy-quark spin-symmetry relation

$$\langle \mathcal{O}^{\chi_{cJ}}[{}^3P_J^{(1)}]\rangle = (2J + 1)\langle \mathcal{O}^{\chi_{c0}}[{}^3P_0^{(1)}]\rangle,$$

which is valid up to $O(v^2)$ corrections.

As it will be shown in Sec. III A below, in the framework of a simplistic GPM-factorization approach described in Sec. II A, the contributions of only color-singlet subprocesses are actually enough to describe small-k_{TC} cross section of J/ψ hadroproduction, but to this end it is important to include both direct and feed-down contributions. There is no room left numerically for the color-octet contributions, and therefore we disregard them entirely in our calculations. This conclusion is perhaps not so surprising, given the fact that color-octet LDMEs are velocity suppressed, as it has been discussed above. Hence, from now on, we will discuss only color-singlet contributions and "NRQCD" labels in our figures below that actually refer to the color-singlet model calculations.

The squared LOs in α_S amplitudes for $2 \to 1$ color-singlet subprocesses in CPM are well known [28],

$$\overline{|\mathcal{A}(g + g \to \mathcal{C}[{}^3P_0^{(1)}])|^2} = \frac{8}{3}\pi^2\alpha_s^2\frac{\langle \mathcal{O}^{\mathcal{C}}[{}^3P_0^{(1)}]\rangle}{M^3}, \tag{24}$$

$$\overline{|\mathcal{A}(g + g \to \mathcal{C}[{}^3P_1^{(1)}])|^2} = 0, \tag{25}$$

$$\overline{|\mathcal{A}(g + g \to \mathcal{C}[{}^3P_2^{(1)}])|^2} = \frac{32}{45}\pi^2\alpha_s^2\frac{\langle \mathcal{O}^{\mathcal{C}}[{}^3P_2^{(1)}]\rangle}{M^3}. \tag{26}$$

As it was discussed above, in GPM, these subprocesses contribute to transverse momentum spectrum because TMD PDFs are involved.

There are two relevant LOs in α_S $2 \to 2$ partonic subprocesses: the first one describes the direct production of J/ψ or $\psi(2S)$ via a color-singlet intermediate state $c\bar{c}[{}^3S_1^{(1)}]$, while in the second one, the $c\bar{c}[{}^3P_1^{(1)}]$ state is produced, which hadronizes to χ_{c1} with a subsequent decay to J/ψ. The squared amplitudes for these partonic subprocess are [34]

$$\begin{aligned}\overline{|\mathcal{A}(g + g \to \mathcal{C}[{}^3S_1^{(1)}] + g|^2} = \pi^3\alpha_s^3\frac{\langle \mathcal{O}^{\mathcal{C}}[{}^3S_1^{(1)}]\rangle}{M^3}\frac{320M^4}{81(M^2 - \hat{t})^2(M^2 - \hat{u})^2(\hat{t} + \hat{u})^2} \\ \times (M^4\hat{t}^2 - 2M^2\hat{t}^3 + \hat{t}^4 + M^4\hat{t}\,\hat{u} - 3M^2\hat{t}^2\hat{u} + 2\hat{t}^3\hat{u} + M^4\hat{u}^2 \\ - 3M^2\hat{t}\hat{u}^2 + 3\hat{t}^2\hat{u}^2 - 2M^2\hat{u}^3 + 2\hat{t}\hat{u}^3 + \hat{u}^4),\end{aligned} \tag{27}$$

$$\overline{|\mathcal{A}(g+g\to\mathcal{C}[^3P_1^{(1)}]+g|^2}=\pi^3\alpha_s^3\frac{\langle\mathcal{O}^{\mathcal{C}}[^3P_1^{(1)}]\rangle}{M^5}\frac{128M^2(\hat{s}\,\hat{u}(\hat{t}+\hat{s})(\hat{u}+\hat{t}))^2}{9(\hat{s}\,\hat{t}(\hat{u}-M^2)(\hat{s}\,\hat{t}+\hat{s}\,\hat{u}+\hat{t}\,\hat{u}))^4}(-15M^2\hat{s}^2\hat{t}^2\hat{u}^2$$
$$+2\hat{s}\,\hat{t}\,\hat{u}\,(-M^8+5M^4(\hat{s}\,\hat{t}+\hat{s}\,\hat{u}+\hat{t}\,\hat{u})+(\hat{s}\,\hat{t}+\hat{s}\,\hat{u}+\hat{t}\,\hat{u})^2)$$
$$+M^2(\hat{s}\,\hat{t}+\hat{s}\,\hat{u}+\hat{t}\,\hat{u})^2(M^4-4(\hat{s}\,\hat{t}+\hat{s}\,\hat{u}+\hat{t}\,\hat{u}))). \tag{28}$$

To calculate the feed-down contribution in prompt J/ψ production, we use following branching ratios which are taken from Ref. [35]: $B(\psi'\to J/\psi+X)=0.614$, $B(\chi_{c0}\to J/\psi+\gamma)=0.014$, $B(\chi_{c1}\to J/\psi+\gamma)=0.343$, and $B(\chi_{c2}\to J/\psi+\gamma)=0.19$, while $B(J/\psi\to\mu^++\mu^-)=0.05961$.

Turning now to the case of CGI-GPM initial-state factorization, we introduce the following notations: $\overline{|\mathcal{A}|^2_{\rm GPM}}$ for the above-described matrix elements of a hard subprocess in the GPM and $H^{(f/d)}_{\rm CGI}$ for the coefficient function, obtained within the CGI-GPM factorization prescription. Then, following Ref. [16], one writes down the contribution of the $2\to1$ or $2\to2$ subprocess of production of $^3P_J^{(1)}$ or $^3S_1^{(1)}$ states of the $c\bar{c}$ pair to the numerator of the TSSA as

$$F_{1T}^{g(f)}\otimes H^{(f)}_{\rm CGI}+F_{1T}^{g(d)}\otimes H^{(d)}_{\rm CGI}==\frac{C_I^{(f)}+C_{F_c}^{(f)}}{C_U}F_{1T}^{g(f)}\otimes\overline{|\mathcal{A}|^2_{\rm GPM}}+\frac{C_I^{(d)}+C_{F_c}^{(d)}}{C_U}F_{1T}^{g(d)}\otimes\overline{|\mathcal{A}|^2_{\rm GPM}}, \tag{29}$$

where $F_{1T}^{g(f)}$ and $F_{1T}^{g(d)}$ are the above-mentioned f-type (C-even) and d-type (C-odd) GSFs, and $\otimes$ denotes convolution in the light-cone momentum fraction and transverse momentum of gluon from the polarized proton. Here C_U is the color factor of the unpolarized cross section, which corresponds to the usual QCD result, while $C_I^{(f/d)}$ and $C_{F_c}^{(f/d)}$ are modified color factors corresponding to ISI and FSI in CGI GPM. In case of a color-singlet state of the $c\bar{c}$ pair, only ISIs (first diagram in Fig. 2) contribute in both cases $^3S_1^{(1)}$ and $^3P_J^{(1)}$, so that $C_{F_c}^{(f)}=C_{F_c}^{(d)}=0$, while it was shown in Refs. [13–18],

$$C_I^{(f)}=-\frac{1}{2}C_U,\qquad C_I^{(d)}=0 \tag{30}$$

for the case of $^3S_1^{(1)}$ final state ($2\to2$ process), while

$$C_I^{(f)}=C_U,\qquad C_I^{(d)}=0 \tag{31}$$

for $^3P_J^{(1)}$ states ($2\to1$ processes). One notices that in both cases d-type GSF does not contribute, so only f-type GSF is relevant for a color-singlet model.

In such a way, accounting for the effects of ISI and FSI with CGI-GPM formalism leads to smaller numerical values of TSSA in charmonium hadroproduction within the color-singlet approximation of NRQCD factorization, as compared to the ordinary GPM.

A comment on the treatment of color-octet contributions in the CGI-GPM approach of Refs. [17,18] is in order here. The authors of Refs. [17,18] had to include contributions of $2\to2$ processes to obtain the nonzero effect on the asymmetry from the color-octet channels. However, e.g., the coefficient function for the contribution of $g+g\to c\bar{c}[^1S_0^{(8)}]+g$ subprocess to the numerator of the asymmetry [Eq. (A3) of Ref. [18]] clearly contains nonintegrable singularities at $\hat{t}\to0$ or $\hat{s}\to m_c^2$ which due to the nonzero transverse momentum of initial-state partons will lead to divergent cross section in GPM. In our opinion, the appearance of nonregulated divergences in CGI-GPM deserves further study and we are going to address this

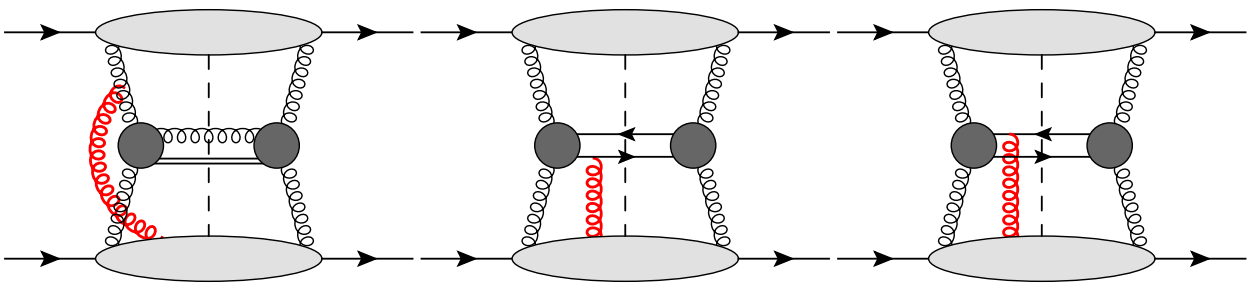

FIG. 2. Example diagrams for contributions to the numerator of TSSA in CGI-GPM. Left panel: ISI for production of $^3S_1^{(1)}$ state. Middle and right panels: FSI for $gg\to c\bar{c}$ process with both final-state quarks tagged.

problem in the future. In the numerical calculations of the present paper, we include only the color-singlet NRQCD channels, which are free from the above-mentioned problem.

C. ICEM

The main physical assumption of the ICEM is that all $c\bar{c}$ pairs with invariant masses below the $D\bar{D}$ threshold hadronize to charmonia with some probability, which is independent from the angular momentum and spin quantum numbers of the $c\bar{c}$ pair. In the ICEM [9,10], the invariant mass of the intermediate charm quark-antiquark pair is constrained to be larger than the mass of the produced charmonium state, $m_{\mathcal{C}}$, instead of using the same lower limit of integration—$2m_c$, as it was done in the traditional CEM [8]. As a result, the ICEM describes the charmonium yields as well as the ratio of $\psi(2S)$ over J/ψ better than the old CEM. The partonic cross section, differential in $c\bar{c}$-invariant mass, is related to the well-known total cross section of production of $c\bar{c}$ pairs as a function of the partonic squared center-of-mass energy $\hat{s}$,

$$\hat{\sigma}(\hat{s}, gg \to c\bar{c}) = \frac{\pi\alpha_S^2}{3\hat{s}}\left[\left(1 + w + \frac{w^2}{16}\right)\ln\left(\frac{1+\sqrt{1-w}}{1-\sqrt{1-w}}\right) - \left(\frac{7}{4} + \frac{31}{16}w\right)\sqrt{1-w}\right],$$
$$\hat{\sigma}(\hat{s}, q\bar{q} \to c\bar{c}) = \frac{8\pi\alpha_S^2}{27\hat{s}}\left(1 + \frac{w}{2}\right)\sqrt{1-w}, \tag{32}$$

with $w = 4m_c^2/\hat{s}$ as follows:

$$\frac{d\hat{\sigma}^{c\bar{c}}}{dM^2} = \hat{\sigma}(\hat{s}, ab \to c\bar{c})\delta(\hat{s} - M^2), \tag{33}$$

so that the GPM-factorization formula for the production of $c\bar{c}$ pairs with invariant mass M and total three-momentum $\mathbf{k}$ via gluon-gluon fusion can be written as

$$\frac{d\sigma^{c\bar{c}}}{dM^2 d^3\mathbf{k}} = \int dx_1 \int d^2q_{1T} \int dx_2 \int d^2q_{2T} F_g(x_1, q_{1T}, \mu_F) F_g(x_2, q_{2T}, \mu_F) \hat{\sigma}(\hat{s}, gg \to c\bar{c}) \times \delta(\hat{s} - M^2)\delta^{(3)}(\mathbf{q}_1 + \mathbf{q}_2 - \mathbf{k}), \tag{34}$$

where the invariant $\hat{s} = k^2 = (q_1 + q_2)^2$ can be represented as in Eq. (8). Finally, for the differential cross section of charmonium $\mathcal{C}$ production in proton-proton collision in ICEM, one has

$$\frac{d\sigma^{\mathcal{C}}}{d^3k} = F_C \times \int_{m_{\mathcal{C}}^2}^{4m_D^2} dM^2 \frac{d\sigma^{c\bar{c}}}{dM^2 d^3k}, \tag{35}$$

where $F_{\mathcal{C}}$ is the process-independent hadronization probability to the charmonium state $\mathcal{C}$. Then one integrates out $\mathbf{q}_{2T}$ and M^2 using delta functions to find

$$\frac{d\sigma^{\mathcal{C}}}{d^3k} = F_{\mathcal{C}} \times \int dx_1 \int d^2q_{1T} \int dx_2 F_g(x_1, q_{1T}, \mu_F) F_g(x_2, q_{2T}, \mu_F) \hat{\sigma}(\hat{s}, gg \to c\bar{c}) \times \delta(q_1^3 + q_2^3 - k^3)[\theta(\hat{s} - m_{\mathcal{C}}^2) - \theta(\hat{s} - 4m_D^2)]. \tag{36}$$

In this equation, the integral over dx_2 can also be removed by the delta function $\delta(q_1^3 + q_2^3 - k^3)$, thus obtaining the master formula for numerical calculations. The quark-antiquark annihilation channel for the $c\bar{c}$-pair production has been incorporated into the calculation in a similar way.

In case of CGI-GPM factorization, the numerator of the TSSA (12) reads as

$$F_{1T}^{g(f)} \otimes \hat{\sigma}_{\mathrm{CGI}}^{(f)}(\hat{s}, gg \to c\bar{c}) + F_{1T}^{g(d)} \otimes \hat{\sigma}_{\mathrm{CGI}}^{(d)}(\hat{s}, gg \to c\bar{c}), \tag{37}$$

where $\hat{\sigma}_{\mathrm{CGI}}^{(f/d)}(\hat{s}, gg \to c\bar{c})$ is the f-/d-type coefficient function of CGI-GPM integrated over the phase space of the final-state $c\bar{c}$ pair with the fixed invariant mass $\hat{s}$ as in Eq. (32). Since in the ICEM both c and $\bar{c}$ quarks in the final state are observed, the corresponding hard-scattering coefficient is different from the coefficient for D-meson TSSA, given, e.g., in Ref. [36].

To obtain new coefficient functions, we take into account interactions of eikonal gluon with the initial-state gluon coming from the unpolarized proton as well as with the final-state $\bar{c}$ and c quarks (middle and right diagrams of Fig. 2). The f-/d-type hard-scattering coefficients thus obtained have the form

$$H^{(f)}_{\mathrm{CGI}}(gg \to c\bar{c}) = \frac{8\pi^2\alpha_s^2}{N_c(N_c^2-1)\tilde{t}^2\tilde{u}^2}(4m_c^4(\tilde{t}+\tilde{u})^2 + 4m_c^2\tilde{t}\,\tilde{u}(\tilde{t}+\tilde{u}) - \tilde{t}\,\tilde{u}\,(\tilde{t}^2+\tilde{u}^2)),$$

$$H^{(d)}_{\mathrm{CGI}}(gg \to c\bar{c}) = N_c\frac{\tilde{t}-\tilde{u}}{\hat{s}}H^{(f)}_{\mathrm{CGI}}(gg \to c\bar{c}),$$

$$H_{\mathrm{CGI}}(q\bar{q} \to c\bar{c}) = -H_{\mathrm{CGI}}(\bar{q}q \to c\bar{c}) = \frac{8\pi^2\alpha_s^2(N_c^2+1)}{\hat{s}^2N_c^2}(2m_c^2\hat{s}+\tilde{t}^2+\tilde{u}^2),$$

where $\tilde{t} = \hat{t} - m_c^2$ and $\tilde{u} = \hat{u} - m_c^2$. Integrating these coefficient functions over the phase space of the final state with the fixed $c\bar{c}$-invariant mass $\hat{s}$, one obtains

$$\hat{\sigma}^{(f)}_{\mathrm{CGI}}(\hat{s}, gg \to c\bar{c}) = \frac{\pi\alpha_S^2}{48\hat{s}}\left[\left(\frac{w^2}{2}-w-1\right)\ln\left(\frac{1-w/2+\sqrt{1-w}}{1-w/2-\sqrt{1-w}}\right) + 2(1+w)\sqrt{1-w}\right], \tag{38}$$

$$\hat{\sigma}^{(d)}_{\mathrm{CGI}}(\hat{s}, gg \to c\bar{c}) = 0, \tag{39}$$

$$\hat{\sigma}_{\mathrm{CGI}}(\hat{s}, q\bar{q} \to c\bar{c}) = \frac{10\pi\alpha_S^2}{27\hat{s}}\left(1+\frac{w}{2}\right)\sqrt{1-w}. \tag{40}$$

It is interesting that the integrated hard-scattering coefficient for d-type GSF is equal to zero similarly to the case of NRQCD, so that in both of our models, a heavy-quarkonium TSSA is sensitive only to f-type GSF.

To obtain prompt-J/ψ production spectra, we take into account direct as well as feed-down contributions from decays of χ_{cJ} and $\psi(2S)$ states. At the stage of numerical calculation in ICEM, we put $m_c = 1.2$ GeV and charmonium masses are taken from PDG tables [35]: $m_{J/\psi} = 3.096$ GeV, $m_{\psi(2S)} = 3.686$ GeV, $m_{\chi_{c0}} = 3.415$ GeV, $m_{\chi_{c1}} = 3.510$ GeV, and $m_{\chi_{c2}} = 3.556$ GeV.

III. NUMERICAL RESULTS

A. PHENIX RHIC

To begin with, we compare the theoretical predictions obtained in the NRQCD-factorization approach with the recent experimental data for the transverse momentum spectra of prompt J/ψ mesons, measured by the PHENIX RHIC experiment [37]. In our NRQCD calculations, we take the charm quark mass as $m_c = m_{\mathcal{C}}/2$, while in the ICEM calculations, it is kept fixed at $m_c = 1.2$ GeV. Also, in the case of feed-down production, the kinematic effect of the mass splittings between the charmonium states turns out to be significant and we take into account the momentum shift between the high-mass charmonium state and the final J/ψ meson as it was done, e.g., in Ref. [38]: $k_{TJ/\psi} = (m_{J/\psi}/m_{\mathcal{C}})k_{T\mathcal{C}}$.

The phenomenological analysis of intrinsic transverse momentum of partons in proton in LO and NLO of CPM [39] demonstrates that for gluon one has $\langle q_T^2\rangle \simeq 1$ GeV^2 and the same estimation was obtained for J/ψ production in GPM [16].

Throughout our analysis, the renormalization and factorization scales have been identified and chosen to be $\mu_F = \mu_R = \xi\sqrt{k_T^2 + m_{\mathcal{C}}^2}$, where ξ varied between $\xi = 1/2$ and $\xi = 2$ about its default value $\xi = 1$ to estimate the theoretical uncertainty due to the freedom in the choice of scales. The resulting errors are indicated as shaded bands in our figures; however, they mostly cancel out in asymmetries A_N.

The direct production of J/ψ mesons at the $O(v^0)$ includes only contributions from CSM (27). The color-octet states $^3P_0^{(8)}$ and $^3P_2^{(8)}$ contribute at $O(v^2)$. The intermediate state $^3P_1^{(8)}$ does not contribute if the initial-state partons are on mass shell. The color-octet contributions $^3S_0^{(8)}$ and $^3S_1^{(8)}$ are suppressed by even higher powers of v, so it is natural to expect them to be negligible at small $k_{T\mathcal{C}} < m_{\mathcal{C}}$. In fact, similarly to the results of Ref. [16], we found that taking into account only the color-singlet production mechanism, the good description of prompt J/ψ transverse momentum spectra at small $k_{TJ/\psi} < m_{J/\psi}$, i.e., in the region of applicability of TMD factorization, can be achieved in the GPM; see the left panel of Fig. 3. Also, our NRQCD calculation leads to the total cross section ratios of direct and feed-down contributions in a good agreement with the experimental data of Ref. [37]; see Table II. However, it should be noted that the relative feed-down contributions of χ_{cJ} states are different in two

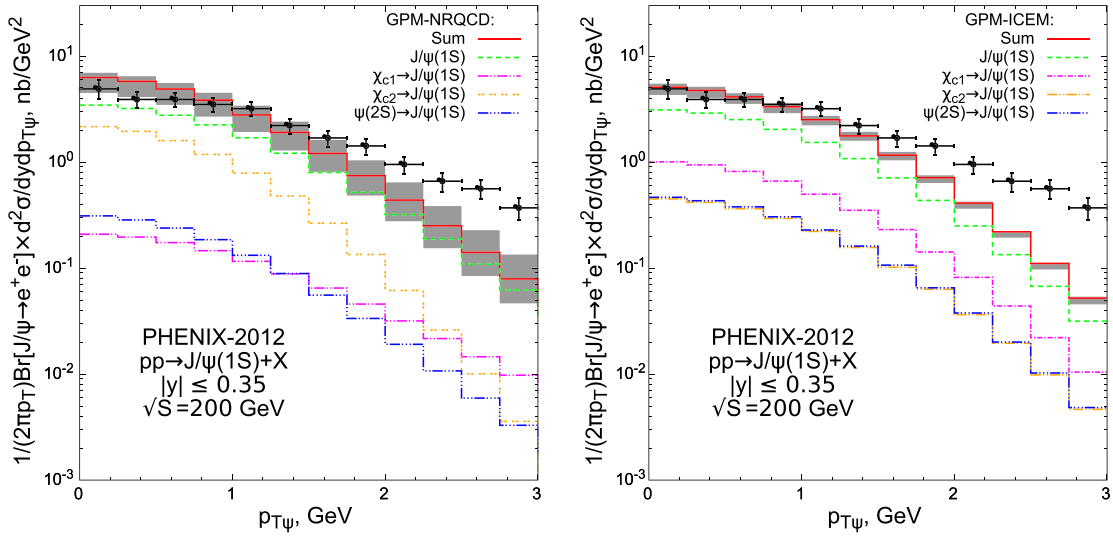

FIG. 3. Differential cross section of prompt J/ψ production as a function of transverse momentum at $\sqrt{s} = 200$ GeV, $|y| < 0.35$. The theoretical results are obtained in GPM with $\langle q_T^2 \rangle = 1$ GeV^2. Left panel: NRQCD-factorization prediction with only color-singlet channels included. Right panel: ICEM prediction. Experimental data are from Ref. [37].

models: in the CSM calculation, χ_{c2} feed-down contributes the most, while in ICEM, the χ_{c1} state is dominant (Fig. 3).

We should emphasize that our calculations are different from calculations of Ref. [16] in the respect that we consistently take into account feed-down contributions from $\psi(2S)$ and χ_{cJ} states, while in Ref. [16] they were added very crudely, by multiplication of the direct cross section by a factor $\simeq$1.4. Such treatment of feed-down is not consistent with the color-singlet model, since the direct J/ψ and $\psi(2S)$ mesons are produced in $2 \to 2$ processes in this model, while χ_{cJ} mesons are produced in $2 \to 1$ processes with significantly different k_{TC} behavior. As one can see from the left panel of Fig. 3, feed-down subprocesses contribute mainly at small transverse momenta in this model. Furthermore, to describe data at large transverse momentum $k_{TJ/\psi}$, $O(k_{TJ/\psi}/m_{J/\psi})$ power corrections are generated in hard scattering by the emission of additional partons, and the inclusion of color-octet contributions in direct charmonium production is absolutely necessary.

Very similar predictions for the transverse momentum spectrum can be obtained in the framework of ICEM; see the right panel of Fig. 3. The values of hadronization probabilities used are $F_{J/\psi} = 0.02$, $F_{\chi_{c1}} = F_{\chi_{c2}} = 0.06$, and $F_{\psi(2S)} = 0.08$. These were obtained via the fit of the total cross section of J/ψ production at PHENIX and the above-mentioned experimentally measured fractions of J/ψ feed-down contribution form $\psi(2S)$ and χ_{cJ} decays (Table II). These values of hadronization probabilities are numerically close to the values obtained in Ref. [10] by the fit of the LHC data in the k_T-factorization approach for the $c\bar{c}$-pair production.

TABLE II. The relative contributions of direct and feed-down production within NRQCD and ICEM. Experimental data of the PHENIX Collaboration for $\sqrt{s} = 200$ GeV are from [37].

$\sqrt{s}$	Model/source of data	$\sigma^{\text{direct}} : \sigma^{\chi_c \to J/\psi} : \sigma^{\psi(2S) \to J/\psi}$
24 GeV	NRQCD	0.58:0.39:0.03
	ICEM	0.68:0.25:0.07
200 GeV	NRQCD	0.61:0.34:0.05
	ICEM	0.61:0.30:0.09
200 GeV	PHENIX Collaboration	0.58:0.32:0.10

Our estimations for TSSAs at PHENIX kinematic conditions, obtained in the GPM accompanied by NRQCD-factorization approach or ICEM, are shown by thin histograms in Fig. 4 and Figs. 5 and 6 as functions of x_F and transverse momentum, respectively, together with the recent experimental data from Ref. [40]. We conclude that within the standard GPM initial-state factorization, the parametrization for the Sivers function by D'Alesio *et al.* is marginally consistent with the experimental data for both hadronization models, while SIDIS1 parametrization predicts too large effects at positive $x_{F\psi}$ and is essentially ruled out for the case of ordinary GPM initial-state factorization.

The TSSA results for the CGI-GPM initial-state factorization are presented in the same Figs. 4–6 by thick histograms. One can see that the discrepancy between the predictions of the CGI-GPM with the SIDIS1 parametrization and experimental data is significantly reduced, rendering it to be reasonably consistent with the experimental data. Another feature of CGI-GPM, evident from Figs. 4–6, is the change of the sign of the TSSA predicted in CGI-GPM relatively to the ordinary GPM.

B. SPD NICA

In this section, we present our predictions for the J/ψ transverse momentum spectrum and TSSA in the kinematic

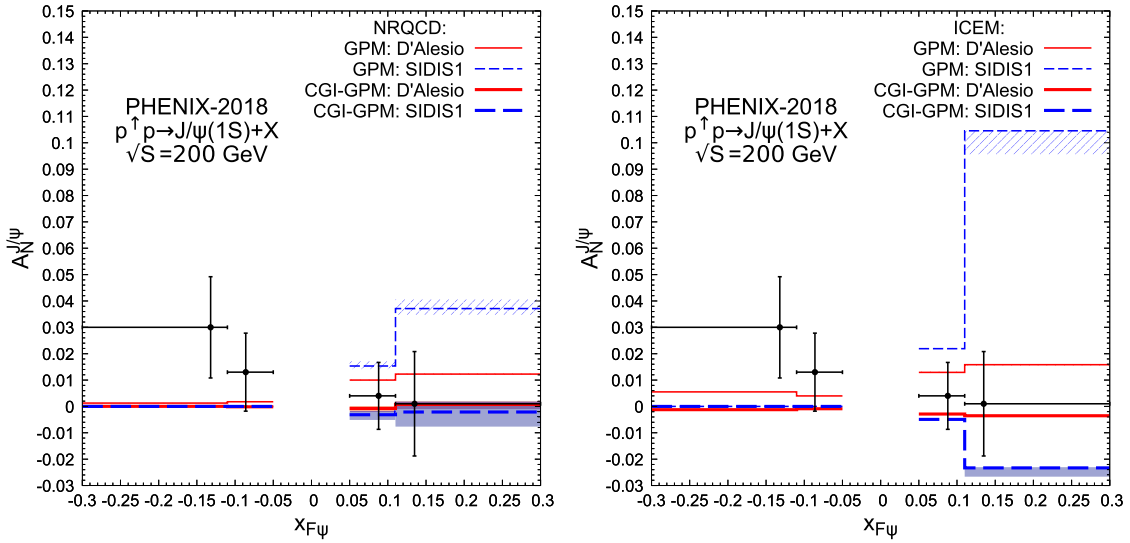

FIG. 4. TSSA $A_N^{J/\psi}$ as function of x_F at $\sqrt{s} = 200$ GeV within the GPM (thin histograms) and CGI-GPM (thick histograms). The theoretical results are obtained with SIDIS1 [6] (dashed histograms) and D'Alesio *et al.* [25] (solid histograms) parametrizations of GSFs. Experimental data are from Ref. [40]. Left panel: NRQCD final-state factorization. Right panel: ICEM final-state factorization.

conditions of a planned SPD NICA experiment in proton-proton collisions with $\sqrt{s} = 24$ GeV. The SPD is expected to be an almost 4π-geometry detector [20,21,41]; thus, a relatively wide coverage in rapidity $|y| < 3$ can be achieved.

As for $k_{TJ/\psi}$ spectrum, the GPM calculations, in both NRQCD factorization and ICEM, lead to results consistent with NRQCD predictions of parton Reggeization approach [42] at a small transverse momentum, while the latter predictions are in agreement with the NLO NRQCD predictions of the collinear parton model [43] at high $k_{TJ/\psi}$, as one can see in the left panel of Fig. 7. Predictions of NRQCD and ICEM approaches for $k_{TJ/\psi}$ spectrum are also remarkably consistent with each other, but ICEM prediction has a smaller scale uncertainty (see the right panel of Fig. 7) because the squared matrix element of the hard process in ICEM is of $O(\alpha_s^2)$ while for NRQCD approach it is of $O(\alpha_s^3)$. The relative contributions of direct

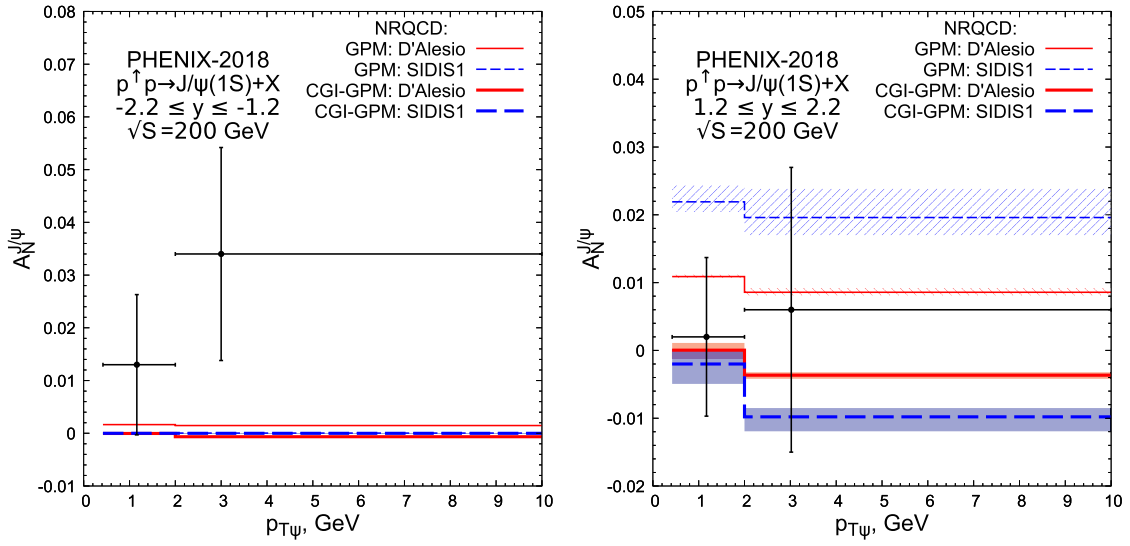

FIG. 5. NRQCD predictions for TSSA $A_N^{J/\psi}$ within the GPM (thin histograms) and CGI-GPM (thick histograms) as a function of J/ψ transverse momentum at $\sqrt{s} = 200$ GeV. The theoretical results are obtained with SIDIS1 [6] (dashed lines) and D'Alesio *et al.* [25] (solid lines) parametrizations of GSFs. Left panel: backward production $(-2.2 < y < -1.2)$. Right panel: forward production $(1.2 < y < 2.2)$. Experimental data are from Ref. [40].

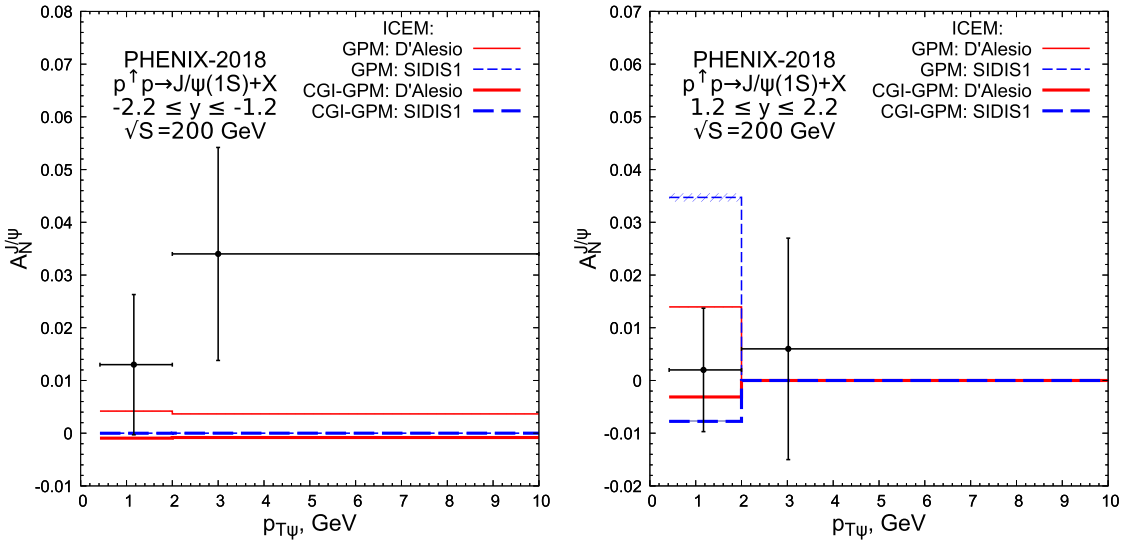

FIG. 6. ICEM predictions for TSSA $A_N^{J/\psi}$ within the GPM (thin histograms) and CGI-GPM (thick histograms) as a function of J/ψ transverse momentum at $\sqrt{s} = 200$ GeV. The theoretical results are obtained with SIDIS1 [6] (dashed lines) and D'Alesio *et al.* [25] (solid lines) parametrizations of GSFs. Left panel: backward production $(-2.2 < y < -1.2)$. Right panel: forward production $(1.2 < y < 2.2)$. Experimental data are from Ref. [40].

and feed-down production at the energy $\sqrt{s} = 24$ GeV are given in Table II and they turn out to be consistent with the PHENIX data. Thus, we conclude that we can safely perform predictions for TSSA at NICA energies.

Estimates for TSSA at SPD NICA experiment computed within NRQCD and ICEM approaches under GPM initial-state factorization assumption are shown in Figs. 8 and 9, respectively, for the SIDIS1 [6] and D'Alesio *et al.* [25] parametrizations for GSF. We find that for standard GPM initial-state factorization, SIDIS1 [6] predicts gigantic values for asymmetries at NICA energies—up to 60% (Fig. 8). However, such big effects can hardly be expected

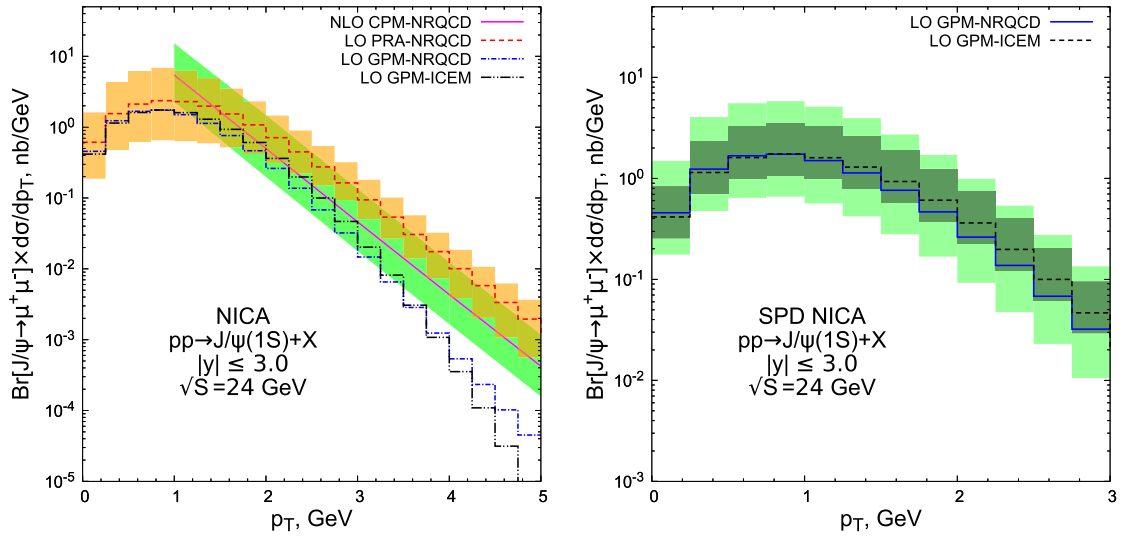

FIG. 7. Prompt J/ψ differential cross section as a function of J/ψ transverse momentum at $\sqrt{s} = 24$ GeV, $|y| < 3$. Left panel: the GPM results with $\langle q_T^2 \rangle = 1$ GeV^2 are shown by the dash-dotted (NRQCD) and dash-double-dotted (ICEM) histograms. Solid and dashed histograms with uncertainty bands are parton Reggeization approach [42] and NLO CPM [43] predictions, respectively. Right panel: the GPM predictions in NRQCD (solid histogram with light green uncertainty band) and ICEM (dashed histogram with dark-green uncertainty band) approaches with their uncertainty bands shown.

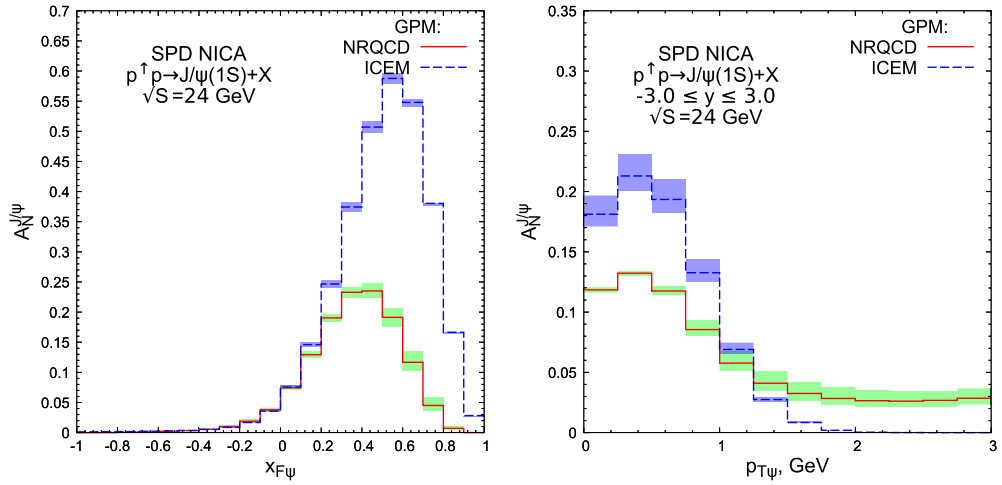

FIG. 8. Comparison of predictions in GPM for TSSA $A_N^{J/\psi}$ as a function of x_F (left panel) and transverse momentum (right panel) at $\sqrt{s} = 24$ GeV in NRQCD (solid histogram) and ICEM (dashed histogram) approaches. The SIDIS1 [6] parametrization of GSFs is used.

to appear, since this parametrization contradicts PHENIX data, when GPM is used. GPM predictions with D'Alesio *et al.* [25] parametrization (Fig. 9) look more realistic and they are quite robust against the choice of J/ψ-formation model. Measurable asymmetries up to 5% for the $x_{F\psi}$ spectrum and up to 2% for $k_{TJ/\psi}$ spectrum are predicted.

Our results obtained using CGI-GPM initial-state factorization are shown in Figs. 10 and 11 for SIDIS1 [6] and D'Alesio *et al.* [25] parametrizations, correspondingly. Similarly to the case of PHENIX kinematics discussed above, the smaller absolute values of TSSAs of charmonium production are predicted within the CGI-GPM factorization in comparison to the usual GPM factorization. Also, in Figs. 10 and 11, within the CGI-GPM+CSM model we observe a sign change of A_N for $p_T \approx 1$ GeV, similar to observations in Ref. [18]. This sign change happens mostly due to a negative color factor in Eq. (30) and a large contribution of direct J/ψ production (see Table II). Another interesting observation is that ICEM predicts only negative values for the TSSA within CGI-GPM, because the integrated coefficient function (38) is negative for $0 \leq w \leq 1$. Finally, from Figs. 10 and 11, one can see that the CSM and the ICEM predict values of the TSSA opposite in sign for SPD NICA kinematic conditions. This potentially allows to discriminate between these two approaches of hadronization within the CGI-GPM, if

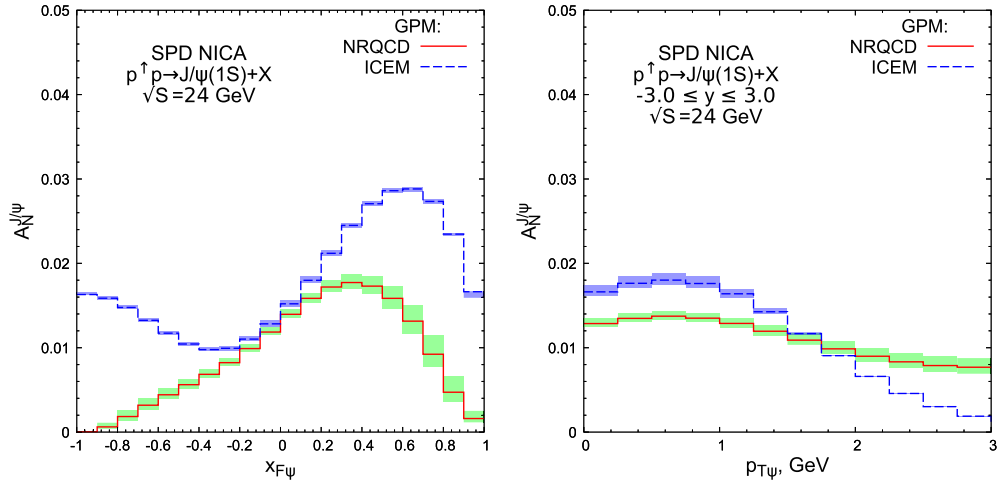

FIG. 9. Comparison of predictions in GPM for TSSA $A_N^{J/\psi}$ as a function of x_F (left panel) and transverse momentum (right panel) at $\sqrt{s} = 24$ GeV in NRQCD (solid histogram) and ICEM (dashed histogram) approaches. The D'Alesio *et al.* [25] parametrization of GSFs is used.

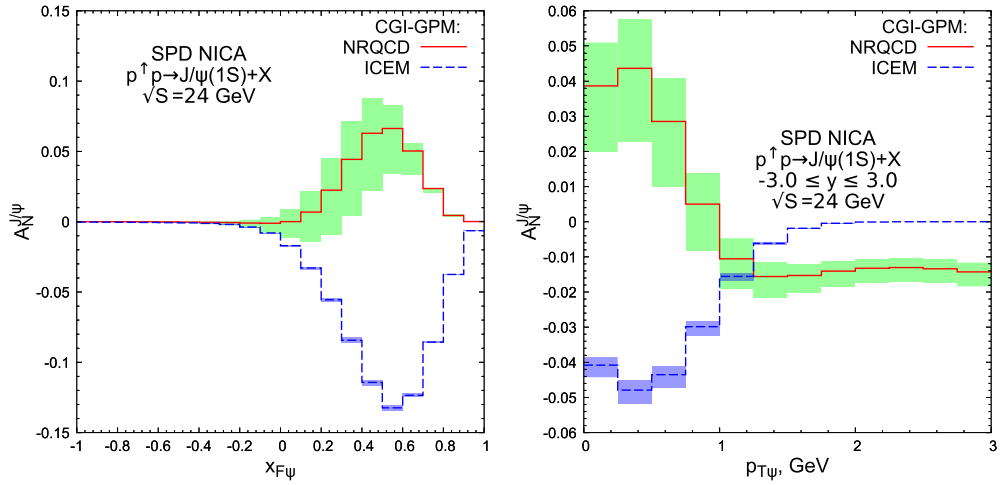

FIG. 10. Comparison of predictions in CGI-GPM for TSSA $A_N^{J/\psi}$ as a function of x_F (left panel) and transverse momentum (right panel) at $\sqrt{s} = 24$ GeV in NRQCD (solid histogram) and ICEM (dashed histogram) approaches. The SIDIS1 [6] parametrization of GSFs is used.

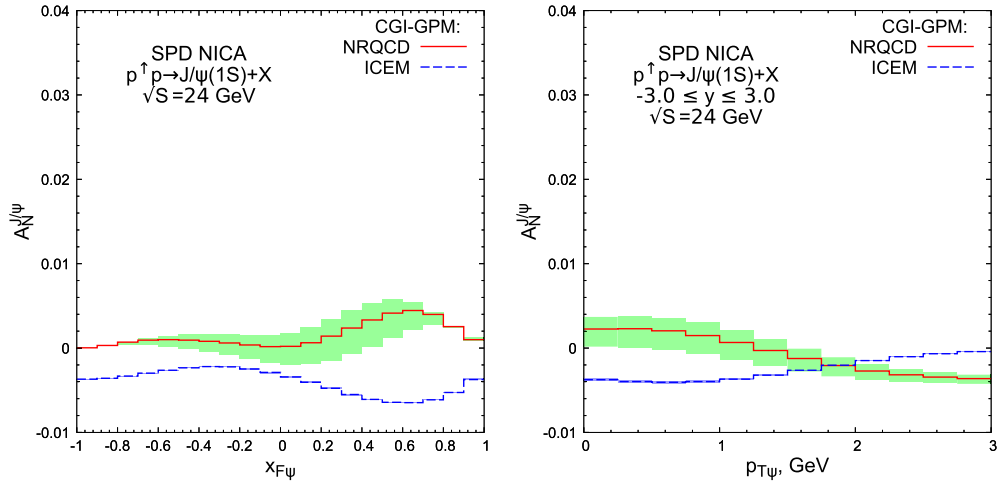

FIG. 11. Comparison of predictions in CGI-GPM for TSSA $A_N^{J/\psi}$ as a function of x_F (left panel) and transverse momentum (right panel) at $\sqrt{s} = 24$ GeV in NRQCD (solid histogram) and ICEM (dashed histogram) approaches. The D'Alesio *et al.* [25] parametrization of GSFs is used.

the energy scan from $\sqrt{s} = 10$ to 27 GeV is performed, allowing to disentangle between the effects of the initial- and final-state factorization.

IV. CONCLUSIONS

In the present paper, we performed a phenomenological analysis of the gluon Sivers function contribution to the transverse TSSA of prompt J/ψ production within NRQCD factorization (essentially the color-singlet model in our case) and ICEM for the description of J/ψ formation, employing both state-of-the-art initial-state factorization models: GPM and CGI-GPM. The goal of our analysis was to make predictions for TSSA in the kinematic conditions of a planned SPD NICA experiment. We found that within the standard GPM initial-state factorization the SIDIS1 parametrization [6] luon Sivers function contradicts PHENIX data, while parametrization of D'Alesio *et al.* [25] leads to reasonable predictions for magnitude, J/ψ transverse momentum, and $x_{F\psi}$ dependence of the asymmetry with $|A_N| \lesssim 2$–3% (Fig. 9). Within the CGI-GPM initial-state factorization, the contradiction of SIDIS1 [6] parametrization with PHENIX data was eliminated, and it predicted $|A_N| \lesssim 5\% - 10\%$ at SPD NICA kinematics (Fig. 10). Hence, the observation of sizable transverse TSSA in inclusive J/ψ production did not contradict the existing experimental data and their theoretical interpretation within a wide range of J/ψ formation and initial-state

factorization models. In any case, measurements at SPD NICA will significantly constrain our knowledge about the gluon Sivers function in a proton.

ACKNOWLEDGMENTS

The authors are grateful to Mathias Butenschön and Bernd Kniehl for providing their NLO CPM predictions for J/ψ transverse momentum spectrum at NICA, to Igor Denisenko, Alexey Guskov, Oleg Teryaev, and other members of the SPD NICA Collaboration, as well as to Gean-Phillipe Lansberg for useful and encouraging physics discussions. The work was supported in parts by the Ministry of Science and Higher Education of Russia via State assignment to educational and research institutions under Project No. FSSS-2020-0014 and by the Foundation for the Advancement of Theoretical Physics and Mathematics BASIS, Grant No. 18-1-1-30-1.

[1] J. C. Collins, D. E. Soper, and G. F. Sterman, Factorization of hard processes in QCD, Adv. Ser. Dir. High Energy Phys. **5**, 1 (1989).
[2] R. Angeles-Martinez *et al.*, Transverse momentum dependent (TMD) parton distribution functions: Status and prospects, Acta Phys. Pol. B **46**, 2501 (2015).
[3] D. W. Sivers, Single spin production asymmetries from the hard scattering of point-like constituents, Phys. Rev. D **41**, 83 (1990).
[4] D. Boer, P. J. Mulders, and O. V. Teryaev, Single spin asymmetries from a gluonic background in the Drell-Yan process, Phys. Rev. D **57**, 3057 (1998).
[5] M. Anselmino, M. Boglione, U. D'Alesio, S. Melis, F. Murgia, and A. Prokudin, Sivers effect and the single spin asymmetry A_N in $p^\uparrow p \to hX$ processes, Phys. Rev. D **88**, 054023 (2013).
[6] U. D'Alesio, F. Murgia, and C. Pisano, Towards a first estimate of the gluon Sivers function from A_N data in pp collisions at RHIC, J. High Energy Phys. 09 (2015) 119.
[7] G. T. Bodwin, E. Braaten, and G. P. Lepage, Rigorous QCD analysis of inclusive annihilation and production of heavy quarkonium, Phys. Rev. D **51**, 1125 (1995).
[8] V. D. Barger, W. Y. Keung, and R. Phillips, On psi and upsilon production via gluons, Phys. Lett. B **91**, 253 (1980); V. D. Barger, W. Y. Keung, and R. Phillips, Hadroproduction of ψ and Υ, Z. Phys. C **6**, 169 (1980); R. Gavai, D. Kharzeev, H. Satz, G. Schuler, K. Sridhar, and R. Vogt, Quarkonium production in hadronic collisions, Int. J. Mod. Phys. A **10**, 3043 (1995).
[9] Y. Q. Ma and R. Vogt, Quarkonium production in an improved color evaporation model, Phys. Rev. D **94**, 114029 (2016).
[10] V. Cheung and R. Vogt, Production and polarization of prompt J/ψ in the improved color evaporation model using the k_T-factorization approach, Phys. Rev. D **98**, 114029 (2018).
[11] M. G. Echevarria, Proper TMD factorization for quarkonia production: $pp \to \eta_{c,b}$ as a study case, J. High Energy Phys. 10 (2019) 144.
[12] S. Fleming, Y. Makris, and T. Mehen, An effective field theory approach to quarkonium at small transverse-momentum, J. High Energy Phys. 04 (2020) 122.
[13] L. Gamberg and Z.-B. Kang, Process dependent Sivers function and implication for single spin asymmetry in inclusive hadron production, Phys. Lett. B **696**, 109 (2011).
[14] U. D'Alesio, L. Gamberg, Z. B. Kang, F. Murgia, and C. Pisano, Testing the process dependence of the Sivers function via hadron distributions inside a jet, Phys. Lett. B **704**, 637 (2011).
[15] U. D'Alesio, F. Murgia, and C. Pisano, Collins and Sivers effects in $p^\uparrow p \to$ jet πX: Universality and process dependence, Phys. Part. Nucl. **45**, 676 (2014).
[16] U. D'Alesio, F. Murgia, C. Pisano, and P. Taels, Probing the gluon Sivers function in $p^\uparrow p \to J/\psi X$ and $p^\uparrow p \to DX$, Phys. Rev. D **96**, 036011 (2017).
[17] U. D'Alesio, F. Murgia, C. Pisano, and S. Rajesh, Single-spin asymmetries in $p^\uparrow p \to J/\psi + X$ within a TMD approach: Role of the color octet mechanism, Eur. Phys. J. C **79**, 1029 (2019).
[18] U. D' Alesio, L. Maxia, F. Murgia, C. Pisano, and S. Rajesh, Process dependence of the gluon Sivers function in $p^\uparrow p \to J/\psi + X$ within a TMD approach in NRQCD, Phys. Rev. D **102**, 094011 (2020).
[19] R. M. Godbole, A. Kaushik, A. Misra, V. Rawoot, and B. Sonawane, Transverse single spin asymmetry in $p + p^\uparrow \to J/\psi + X$, Phys. Rev. D **96**, 096025 (2017).
[20] I. A. Savin, A. V. Efremov, D. V. Peshekhonov, A. D. Kovalenko, O. V. Teryaev, O. Y. Shevchenko, A. P. Nagajcev, A. V. Guskov, V. V. Kukhtin, N. D. Topilin, A. Efremov, D. Peshekhonov, A. Kovalenko, O. Teryaev, O. Shevchenko, A. Nagajcev, A. Guskov, V. Kukhtin, and N. Toplilin, Spin Physics Experiments at NICA-SPD with polarized proton and deuteron beams, EPJ Web Conf. **85**, 02039 (2015).
[21] A. Arbuzov, A. Bacchetta, M. Butenschoen, F. G. Celiberto, U. D'alesio, M. Deka, I. Denisenko, M. G. Echevarria, A. Efremov, and N. Y. Ivanov *et al.*, On the physics potential to study the gluon content of proton and deuteron at NICA SPD, Prog. Part. Nucl. Phys. **119**, 103858 (2021).
[22] J. Collins, Foundations of Perturbative QCD (Cambridge University Press, Cambridge, 2011).
[23] A. Vladimirov, TMD evolution as a double-scale evolution, Proc. Sci., SPIN2018 (**2019**) 054.
[24] A. Bacchetta, U. D'Alesio, M. Diehl, and C. A. Miller, Single-spin asymmetries: The Trento conventions, Phys. Rev. D **70**, 117504 (2004).

[25] U. D'Alesio, C. Flore, F. Murgia, C. Pisano, and P. Taels, Unraveling the gluon Sivers function in hadronic collisions at RHIC, Phys. Rev. D **99**, 036013 (2019).
[26] S. J. Brodsky, D. S. Hwang, and I. Schmidt, Final state interactions and single spin asymmetries in semiinclusive deep inelastic scattering, Phys. Lett. B **530**, 99 (2002).
[27] E. J. Eichten and C. Quigg, Quarkonium wave functions at the origin, Phys. Rev. D **52**, 1726 (1995).
[28] P. L. Cho and A. K. Leibovich, Color octet quarkonia production, Phys. Rev. D **53**, 150 (1996).
[29] P. L. Cho and A. K. Leibovich, Color octet quarkonia production. 2., Phys. Rev. D **53**, 6203 (1996).
[30] M. Butenschoen and B. A. Kniehl, World data of J/ψ production consolidate NRQCD factorization at NLO, Phys. Rev. D **84**, 051501 (2011).
[31] B. A. Kniehl, D. V. Vasin, and V. A. Saleev, Charmonium production at high energy in the k_T -factorization approach, Phys. Rev. D **73**, 074022 (2006).
[32] V. A. Saleev, M. A. Nefedov, and A. V. Shipilova, Prompt J/ψ production in the Regge limit of QCD: From Tevatron to LHC, Phys. Rev. D **85**, 074013 (2012).
[33] R. Barbieri, M. Caffo, R. Gatto, and E. Remiddi, QCD corrections to P wave quarkonium decays, Nucl. Phys. **B192**, 61 (1981).
[34] R. Gastmans, W. Troost, and T. T. Wu, Cross sections for gluon + gluon → heavy quarkonium + gluon, Phys. Lett. B **184**, 257 (1987).
[35] P. A. Zyla *et al.* (Particle Data Group), Review of particle physics, Prog. Theor. Exp. Phys. **2020**, 083C01 (2020).
[36] C. Pisano, U. D'Alesio, C. Flore, F. Murgia, and P. Taels, Process dependence of the gluon Sivers function in inclusive pp collisions: Theory, Proc. Sci., SPIN2018 (**2019**) 048.
[37] A. Adare *et al.* (PHENIX Collaboration), Ground and excited charmonium state production in $p + p$ collisions at $\sqrt{s} = 200$ GeV, Phys. Rev. D **85**, 092004 (2012).
[38] B. A. Kniehl, M. A. Nefedov, and V. A. Saleev, $\psi(2S)$ and $\Upsilon(3S)$ hadroproduction in the parton Reggeization approach: Yield, polarization, and the role of fragmentation, Phys. Rev. D **94**, 054007 (2016); H. S. Shao, H. Han, Y. Q. Ma, C. Meng, Y. J. Zhang, and K. T. Chao, Yields and polarizations of prompt J/ψ and $\psi(2S)$ production in hadronic collisions, J. High Energy Phys. 05 (2015) 103.
[39] C. Y. Wong and H. Wang, Effects of parton intrinsic transverse momentum on photon production in hard scattering processes, Phys. Rev. C **58**, 376 (1998).
[40] C. Aidala *et al.* (PHENIX Collaboration), Single-spin asymmetry of J/ψ production in $p + p$, $p +$ Al, and $p +$ Au collisions with transversely polarized proton beams at $\sqrt{s_{NN}} = 200$ GeV, Phys. Rev. D **98**, 012006 (2018).
[41] V. M. Abazov, V. Abramov, L. G. Afanasyev, R. R. Akhunzyanov, A. V. Akindinov, N. Akopov, I. G. Alekseev, A. M. Aleshko, V. Y. Alexakhin, and G. D. Alexeev *et al.*, Conceptual design of the spin physics detector, arXiv: 2102.00442.
[42] A. V. Karpishkov, M. A. Nefedov, and V. A. Saleev, Spectra and polarizations of prompt J/ψ at the NICA within collinear parton model and parton Reggeization approach, J. Phys. Conf. Ser. **1435**, 012015 (2020).
[43] M. Butenschön and B. A. Kniehl (to be published).